

Certain Features of UHF Propagation during Solar Proton Events

Yu. V. Goncharenko^a, F. V. Kivva^a, and V. G. Gutnik^b

^a *Usikov Institute of Radiophysics and Electronics, National Academy of Sciences of Ukraine, ul. Akademika Proskury, Kharkov, 61085 Ukraine*
e-mail: YGonch@ire.kharkov.ua

^b *Institute of Radioastronomy, National Academy of Sciences of Ukraine, Krasnoznamenaya ul. 4, Kharkov, 61002 Ukraine*
e-mail: gutnik@rian.kharkov.ua

Received November 26, 2004; in final form, July 5, 2005

Abstract—Results of the experimental reception of the UHF signal from geostationary satellite, visible at a low elevation angle from the receiving point, have been considered. It has been noted that the fluctuation intensity considerably increases during powerful solar proton events. The observed effect can be caused by interference between direct and secondary rays related to tropospheric irregularities. The hypothesis explaining obtained results based on the optical model of solar–tropospheric coupling is proposed.

PACS numbers: S94.20.Bb

DOI: 10.1134/S0016793206020137

1. INTRODUCTION

As a result of intense development of different-purpose radio systems operating in the UHF band (satellite radio communication and navigation, radar systems of different types, ground-based communication facilities, etc.), to the reliability of which increased demands are made, it became necessary to experimentally study the conditions of radio propagation in unusual situations, e.g., during solar flare events and related magnetic storms. In the years of increased solar activity, the number of geomagnetically disturbed days can reach 10–15% of the total time [*Solar ...*, 2003]. In such a situation the statistical characteristics of UHF signals from telecommunication and navigation satellites received by ground-based stations can considerably differ from the known characteristics obtained in the absence of solar flares [Salonen et al., 1996]. To obtain this information, it is necessary to systematically measure the level of UHF signals emitted by satellites during solar flares of different intensity.

2. EXPERIMENTAL TECHNIQUE

The signal from the AsiaSat-3S geostationary telecommunication satellite (the orbital position 105°), visible from the receiving point (Kharkov) at an elevation angle of about 4.5° and an azimuth of 72° (received signal frequency is 3610 MHz), was analyzed during the experiments. The calibration signal (CS) was generated in the receiving channel in order to completely amplify the system. As a result, the error of amplitude measure-

ments decreased to 0.3–0.5 dB. The received signal level was registered at a frequency of 1 Hz.

The measurements were performed from the end of April 2002 to the end of November 2003 in series of duration 6–10 days and at an interval between the series not longer than 4 days. The total duration of the measurements was 405 days, which accounts for 67.5% of the entire experimental period.

Twenty three solar proton events (SPEs) of different intensity, during which the solar particle density and velocity increased and the geomagnetic field became disturbed (magnetic storm), were registered in the course of measurements. The received signal intensity was measured during 16 SPEs, which accounts for

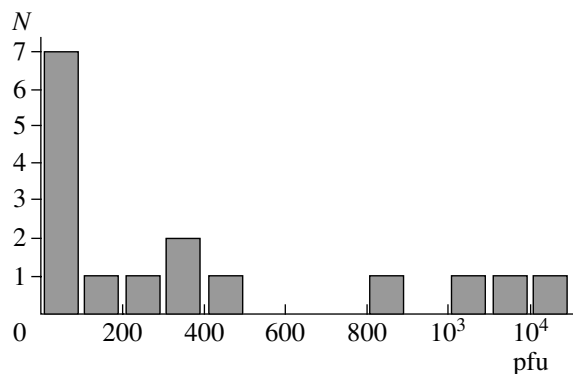


Fig. 1. Distribution of SPEs during which the pfu values were determined.

$\approx 70\%$ of the total number of occurred proton events. Figure 1 shows the SPE distribution with respect to the maximal increase in the flux density of high-energy solar protons relative to the undisturbed state (in proton flux units, pflu), during which the signal was received, constructed based on [Solar ..., 2003] data.

The energy spectrum of solar protons during SPEs can considerably change depending on the SPE phase and class. The estimates indicate that, at latitudes of 50° – 55° in the upper troposphere, the flux of high-energy solar protons can become commensurable with that of galactic protons only during SPEs with pflu ≈ 200 – 300 .

The variations in the received signal parameters were studied independently for six powerful SPEs with pflu > 300 and for six arbitrarily selected weak SPEs with pflu < 300 .

3. DATA PROCESSING AND ANALYSIS

The signal characteristics a day before, during, and after the flare averaged for 1 h were statistically analyzed. The superposed epoch method, where the time of high-energy solar proton (solar cosmic rays, SCRs) registration in the Earth orbit was taken as an origin, was used in data processing.

The experiment indicated that the variations in the signal level related to a change in meteorological conditions (rain, snow, fog, dense clouds) can reach 10–15 dB, whereas the variations in the average signal value obtained during powerful solar flares did not exceed 1–2 dB. Therefore, a change in the average signal level is not a convincing indicator of the effect of solar activity on the communication channel parameters.

An analysis of the signal amplitude distribution law indicated that an insignificant change in the amplitude average value is related to fading events which appear during a solar flare. Therefore, it seems reasonable to consider these events as a random impulsive process. For this process the main quantities characterizing fading statistics are depth, duration, recurrence frequency or the interval between adjacent fading events, and fading occurrence probability.

Figure 2 shows the fading depth probability below the registered value $y - P(y)$, depending on time during weak SPE. It is clear that the occurrence probability of fading with a depth of 4 dB is not higher than 0.01, and fading events with a depth of 6 dB and more are almost not observed. This agrees with the results obtained by Salonen et al. [1996], who demonstrated that the fluctuation effects with a depth of 2 dB and more are observed in the UHF band on slightly inclined paths during not more than 1% of time. Consequently, based on the obtained experimental data, it is impossible to estimate the effect of weak SPEs on the parameters of the geostationary satellite–Earth communication channel.

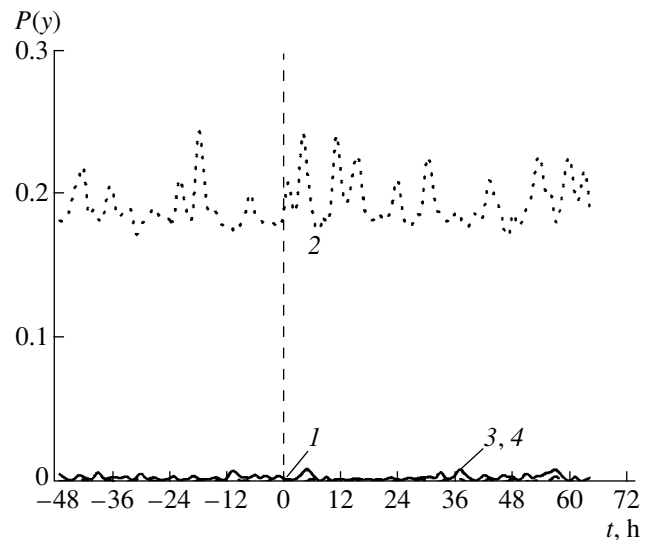


Fig. 2. The probability of a decrease in the signal amplitude below the registered value $P(y)$ depending on time during a weak solar flare: (1) solar flare beginning; (2–4) the probabilities of a decrease in the signal below the levels (y) equal to -2 , -4 , and -6 dB as compared to the average value.

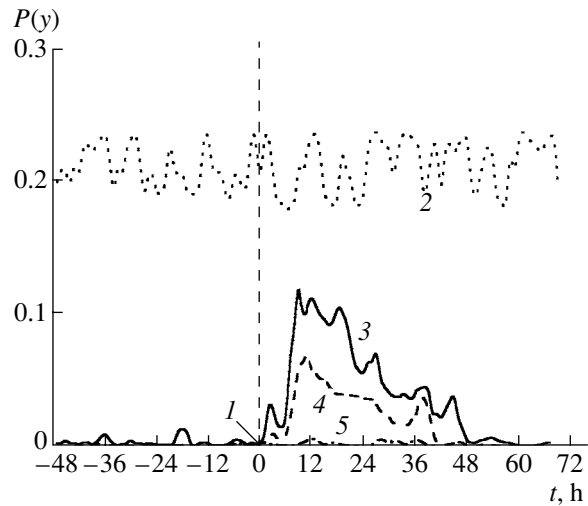


Fig. 3. The probability of a decrease in the signal amplitude below the registered value $P(y)$ depending on time during a strong solar flare: (1) solar flare beginning; (2–5) the probabilities of a decrease in the signal below the levels (y) equal to -2 , -4 , -6 , and -9 dB as compared to the average value.

After the beginning of a powerful solar flare with pflu > 300 , the probability that the signal amplitude decreases by 4 dB increased by a factor of 3–6 and sometimes reached 0.09 (see Fig. 3). In this case the probability of signal decrease by 6 dB increased to 0.02, i.e., by almost an order of magnitude. These effects can be explained by a considerable increase in the number of deep fading per unit time 4–6 h after the beginning of SCR registration in the Earth orbit. The

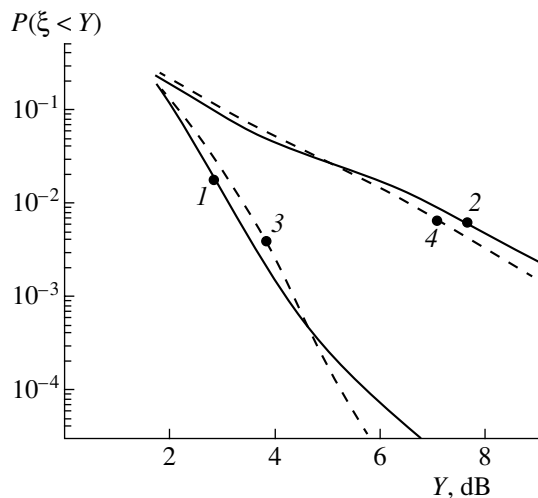


Fig. 4. Integral distribution laws of received signal fluctuations: (1) before SPE, (2) during SPE, (3) the normal distribution law, and (4) the distribution law of the form $P(\xi < Y) \sim Y^4$.

dynamics of variations in the signal intensity acquires the initial, preflare, form 66–72 h after the flare beginning.

When radio waves propagate in the atmospheric communication channel, the received signal distribution law can be described by the generalized Rayleigh law in most cases [Lectures..., 1964]. However, if turbulence is isotropic in the region substantial for radio propagation and local formations are absent (i.e., a direct signal is much larger than secondary signals reflected from or refracted by these formations), the generalized Rayleigh law can be replaced by the Laplace–Gauss law or by the normal distribution law [Kalinin and Cherenkov, 1971]. Figure 4 presents the integral distribution laws for the received signal fluctuations before and during powerful SPEs. In the absence of SPEs, the fluctuation distribution law can be approximated by the normal distribution law, which indicates that many commensurable irregularities are present on a path and the level of signals related to these irregularities is low. After the beginning of a strong solar flare, the fluctuation spectrum changes due to the appearance of fast fading and can be approximated by the generalized Rayleigh law or by the distribution power law of the form $P(\xi < Y) \sim Y^4$. Such a law can characterize a multiray wave propagation on paths with a small number (less than five) of secondary reflectors [Gorbach et al., 2002].

The assumption of an interference origin of fading is also confirmed when received signal realizations are considered in detail. Figure 5 indicates that the appeared fading events of duration 10–30 s (position 3 in Fig. 5) have a sharp minimum, whereas the received signal intensity increases smoothly, which is typical of interference fading. Approximately two days later, the

depth and frequency of the described fading events decrease to the initial, preflare, value.

4. DISCUSSION OF RESULTS

The characteristic feature of the received signal consists in that the signal fluctuations increase some time after the solar flare. This can be related to either underlying surface, or radio signal source, or propagation medium (the ionosphere and troposphere).

A change in the statistical characteristics of a received signal can be explained by variations in the underlying surface parameters. As a result of interference between direct waves and waves reflected from the Earth's surface, the resultant signal can exert fading registered in the described experiment. In this experiment the wave reflected from the underlying surface is weakened by the receiving antenna pattern by 5–10 dB depending on the angle of arrival. Thus, the fading depth related to a change in the underlying surface properties cannot exceed 3–5 dB, and the fading duration is usually several minutes. The duration of fading registered during the experiment is not more than 20–30 s, and the fading depth reaches 9 dB. Consequently, changes in the underlying surface properties cannot substantially affect received signal amplitude fluctuations.

When signal is received from geostationary satellite visible from a receiving point at a small elevation angle, the length of the ionospheric path leg can reach 2–3 thousand kilometers. When propagating in the plasma that is located in the geomagnetic field, the polarization plane of a linearly polarized electromagnetic wave turns, and this turn depends on the geomagnetic field strength and electron density (the Faraday effect). Changes in the polarization plane can cause a decrease in the signal level registered in the course of the experiment. The dependence of the polarization plane turning angle on the ionospheric parameters can be represented in the form [Grigorenko, 1979]:

$$\Omega = 2.98 \times 10^{-2} f_0^{-2} \int_0^L M(l) N_e(l) dl, \quad (1)$$

where Ω is the polarization plane turning angle, rad; f_0 is the electromagnetic radiation frequency, Hz; L is the ionospheric path length, m; $M(l)$ is the longitudinal component of the geomagnetic field, A m⁻¹; $N_e(l)$ is the electron density profile along the path, m⁻³; and $N_H = \int_0^L N_e(l) dl$ is the total electron content in a unit column.

The calculations performed by Grigorenko [1979] indicate that the total electron content (TEC) in a unit column, directed along a tangent to the Earth's surface (which insignificantly differs from the considered case), at a maximum of solar activity is $\sim 10^{18}$ m⁻². Proceeding from this value and expression (1), we can determine that the diurnal turn of the polarization plane

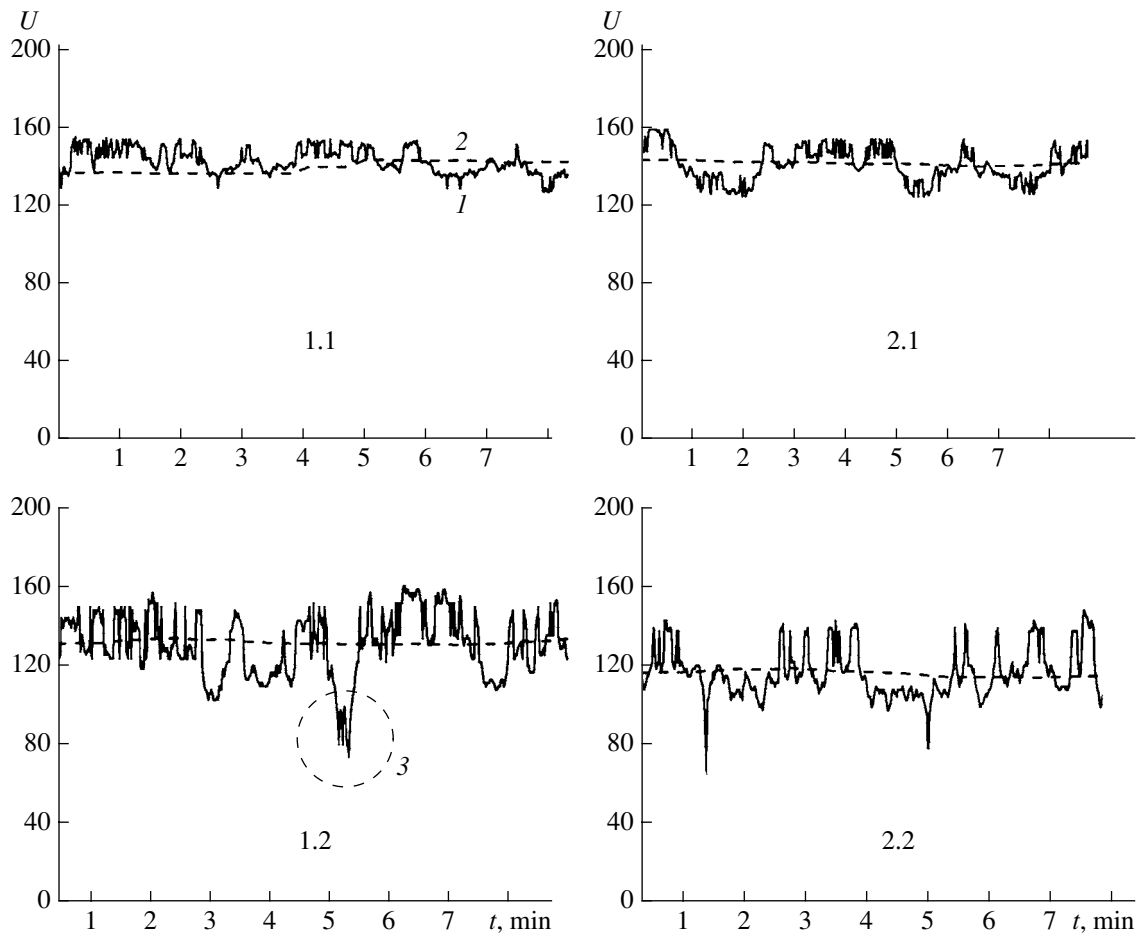


Fig. 5. Variations in the received signal level during solar flares of November 9, 2002 (1.1–1.4) and October 30, 2003 (2.1–2.4) 8 h before the flare beginning (1.1, 1.2) and 4 h after the flare beginning (1.2, 2.2).

of the electromagnetic wave with a frequency of ~ 4 GHz is not more than 15° – 20° even at a maximum of solar activity. In this case the maximal rate of a change in the turning angle cannot be higher than 5° – 10° per hour proceeding from the maximal rate of a change in TEC. That is, fading related to the Faraday effect cannot exceed 0.5–1 dB.

The fading intensity increases registered experimentally can result from interference between the direct wave and the waves related to the ionospheric E and E_s layers, where the electron density can considerably change. Thus, the calculations indicate that the maximal electron density contribution to a change in the refraction coefficient of the medium at a frequency of ~ 4 GHz can exceed 0.5–0.75 units of N for the E layer and 1.5–2 units of N for the E_s , F_1 , and F_2 layers. However, in the practice the space–time variations in the refraction coefficient are lower by a factor of 5–10 [Fatkullin et al., 1981] and cannot substantially affect UHF propagation.

The estimates indicate that an increase in TEC by a factor of 10 and more 30–60 min after the solar flare beginning [Grigorenko, 1979] leads to a decrease in the

refraction coefficient of the ionosphere and to a change in the path electric length, which can reach 10 – 15λ . This can result in a change in the radio propagation trajectory and in the appearance of deep fading, which should be taken into account when analyzing the obtained experimental data.

In addition to the possible effect of the ionosphere, we will subsequently consider the statistical characteristics of a received signal changed as a result of a change in the signal propagation conditions in the troposphere.

The passage of strong atmospheric fronts, which make the troposphere more unstable, through the zone of the experimental path can also cause considerable fluctuations of a received signal. An analysis of the meteorological data related to each of six powerful flares indicated that a passage of atmospheric fronts was not registered in any of the considered cases. Figure 6 presents the variations in the cloud cover density and atmospheric pressure two days before, during, and after the strong solar flare obtained using the superposed epoch method.

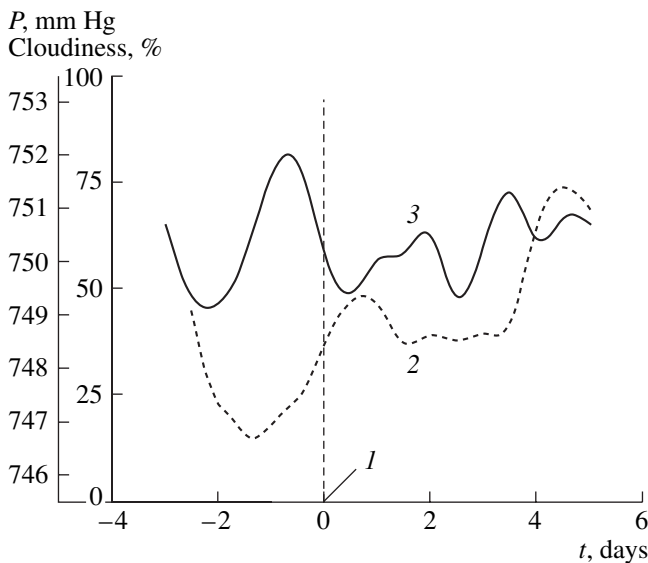


Fig. 6. Variations in the meteorological parameters during a strong solar flare: (1) SPE beginning, (2) atmospheric pressure, and (3) cloud cover density.

An analysis of the data presented in Fig. 3 indicates that the product of the solar flare affecting the troposphere reaches this region for not more than 4–8 h. It is known that the total irradiance (solar constant) weakly depends on solar flare activity, and the activity variations are not more than 0.2% [The Solar..., 1977]. However, a change in the energy flux in the UV and X-ray bands, as well as in the corpuscular part of the solar spectrum, can exceed 1000%. Therefore, variations in the radio propagation conditions on the geostationary satellite–Earth path can be caused by increased HF (UV, X-ray) irradiances that reach the Earth for approximately 8 min or by the variations in the flux of high-energy solar cosmic particles or rays.

At present, one of the main models of solar–terrestrial coupling is the optical model [Avdyushin and Danilov, 2000]. According to this model, the GCR and SCR fluxes stimulate the course of chemical reactions in the atmosphere and govern the NO content. The concentration of NO is responsible for the amount of NO₂ and O₃ in the atmosphere affecting the state of the atmosphere. Other mechanisms of the effect of SCR variations on the meteorological parameters of the troposphere can also exist within the scope of this model.

Taking into account that solar protons with energies higher than 300–400 MeV generated during SPEs appear in the Earth's atmosphere 1–2 h after the flare beginning, and the solar wind density and velocity near the Earth orbit increase only 2–3 days later, we can state that high-energy solar proton fluxes are to a certain degree preferable in verifying the model of the effect of solar activity on the radio propagation path parameters. When reaching the Earth's atmosphere, these fluxes can ionize atmospheric gases. Thus, one

more ionization source (SCRs) can be added to the main ionization source in the upper troposphere (GCRs) during solar flares. In this case the ionization rate at an altitude of 10 km can increase by a factor of 5–10 [Bryant et al., 1967]. Produced ions can be water vapor nuclei even in the absence of supersaturation since the equilibrium water vapor pressure over the surface of a charged drop is lower than over an uncharged drop surface [Das Gupta and Ghosh, 1947]. Microscopic water drops of 5 μm and smaller in diameter can exist at altitudes of about 8 km in the upper troposphere at a temperature of –30°C for several tens of hours not being frozen, whereas coarser drops exist at such temperatures for only several seconds [Scorer, 1980]. The experimental data [Titlov and Baum, 1993] indicate that layers with increased water vapor content were found out at altitudes of 7–10 km. In this case the refraction coefficient component related to water vapor can reach 4–5 units of *N* at an altitude of 8 km. A preliminary analysis performed by us [Goncharenko and Kivva, 2002] indicated that such layers cannot directly affect the radio propagation conditions but can lead to a change in the temperature profile of the middle and upper troposphere registered in [Pudovkin and Dement'eva, 1997]. As a result, the probability of mass transfer from the stratosphere into the upper troposphere considerably increases [Reiter, 1978]. Turbulent formations of a cat eye type, the mechanism of formation and development of which was described in [Scorer, 1980], can appear at the boundary between the tropospheric and intruded stratospheric air. The refraction coefficient of intruded air is lower by 4–10 units of *N* than in the ambient troposphere. Consequently, such irregularities can affect UHF radio propagation. The estimates indicate that the difference between the direct wave and the wave refracted by such irregularities is 0.2–0.4 λ, which can be sufficient for the appearance of fading registered in the considered experiment.

Solar electrons, low-energy solar protons, and other particles (the solar wind) penetrate into the Earth's magnetosphere 48–72 h after a solar flare. As a result, the geomagnetic field becomes disturbed (magnetic storm appears). One of the effect related to magnetic storms is the Forbush effect, when the GCR flux density near the Earth's surface decreases by 10–20% and, sometimes, by 50%. The data on the SCR flux density obtained on the NOAA geostationary satellites indicate that the amount of protons with energies higher than 300–400 MeV 2–3 days after the flare beginning is almost equal to such an amount before flare. Thus, the intensity of both ionization sources in the atmosphere considerably decreases 48–72 h after the flare beginning. The ion density and the related aerosol density in the upper troposphere fall, which finally results in a considerable decrease in the probability of penetration of stratospheric air masses into the troposphere. Figure 3 indicates that the disturbance of the troposphere in not more than three days after the solar flare beginning decreases to the initial level. This confirms the hypoth-

esis that SCRs are related to irregularities in the upper troposphere.

Variations in the received signal structure were sometimes registered in the absence of solar flares. However, the occurrence probability of such changes did not exceed 0.04–0.06 in the absence of solar flares, whereas each powerful proton event was accompanied by the described intensity changes of different intensity.

5. CONCLUSIONS

An analysis of the experimental data indicated that solar proton events cause an increase in the fluctuation intensity of a received satellite signal. This can result from interference between the direct wave and the secondary waves related to turbulent irregularities in the upper troposphere. Such turbulent formations can accompany stratospheric air flows penetrating into the troposphere during SPEs. The proposed mechanism of the effect of solar energetic events on the upper troposphere does not contradict the obtained experimental data and makes the previously known optical model of solar–terrestrial coupling more complete.

REFERENCES

1. S. I. Avdyushin and A. D. Danilov, "The Sun, Weather, and Climate: A Present-Day View of the Problem (Review)," *Geomagn. Aeron.* **40** (5), 3–14 (2000) [*Geomagn. Aeron.* **40**, 545–555 (2000)].
2. D. A. Bryant, T. L. Cline, U. D. Desai, and F. B. McDonald, "Explorer 12 Observations of Solar Cosmic Rays and Energetic Storm Particles after the Solar Flare of September 28, 1961," *J. Geophys. Res.*, 4983–4989 (1967).
3. N. N. Das Gupta and S. K. Ghosh, "A Report on the Wilson Cloud Chamber and Its Applications in Physics," *Rev. Mod. Phys.* **18** (12) (1946).
4. M. N. Fatkullin, T. I. Zelenova, V. K. Kozlov, et al., *Empirical Models of the Midlatitude Ionosphere* (Nauka, Moscow, 1981) [in Russian].
5. Yu. V. Goncharenko and F. V. Kivva, "On Dimensions of Atmospheric Aerosol Particles in Reflecting Layers That Appear after Strong Solar Flares," *Radiofiz. Elektron.* **7** (3), 509–512 (2002).
6. N. V. Gorbach, L. I. Sharapov, and V. G. Gutnik, "Specific Features of Statistical Characteristics of 3-mm Radiowaves during Propagation above Rough Sea Surface," *Radiofiz. Radioastron.* **7** (1), 5–10 (2002).
7. E. I. Grigorenko, "Studies of the Ionosphere Based on the Faraday Effect Observations during Incoherent Radiowave Scattering," *Ionos. Issled.*, No. 27, 60–73 (1979).
8. A. I. Kalinin and E. L. Cherenkova, *Radio Propagation and Radio Line Operation* (Svyaz', Moscow, 1971) [in Russian].
9. *Lectures on Communication System Theory*, Ed. by E. Dzh. Bagdadi, (Mir, Moscow, 1964).
10. M. I. Pudovkin and A. L. Dement'eva, "Variations of the Temperature Altitude Profile in the Lower Atmosphere during Solar Events," *Geomagn. Aeron.* **37** (3), 84–91 (1997) [*Geomagn. Aeron.* **37**, 321–325 (1997)].
11. R. Reiter, "Increased Influx of Stratospheric Air into the Lower Troposphere after Solar H and X-Ray Flares," *J. Geophys. Res.* **78**, 6167 (1978).
12. Erkki T. Salonen, Jouni K. Terveonen, and W. J. Vogel, "Scintillation Effects on Total Fade Distribution for Earth–Satellite Links," *IEEE Trans. Antennas Propag.*, No. 1, 23–27 (1996).
13. R. S. Scorer, *Environmental Aerodynamics* (Horwood, Chichester, 1978; Mir, Moscow, 1980).
14. *Solar Proton Events Affecting the Earth Environment. January 1976–September, 20, 2003* (US Report, Department of Commerce, NOAA, Space Environment Center, 2003).
15. *The Solar Output and Its Variations*, Ed. by O. R. White (Boulder, 1977; Mir, Moscow, 1980).
16. J. Titlow and B. A. Baum "Atmospheric Parameterization Schemes for Satellite Cloud Property Retrieval during FIRE IFO II," in *Proceedings of the Conference Sponsored by the NASA, the NSF, the NOAA, the Department of Energy, and the Office of Naval Research, Breckenridge, 1993*, pp. 83–86.